Tenth U.S. National Conference on Earthquake Engineering
Frontiers of Earthquake Engineering
July 21-25, 2014
Anchorage, Alaska

STUDY OF THE IMPACT OF A MAGNITUDE 9.0 CASCADIA SUBDUCTION ZONE EARTHQUAKE ON BRITISH COLUMBIA, CANADA

A. Nasseri[1], M. Turel[2], Y. Yin and T. Lai[3]

ABSTRACT

The need for assessing potential impact of catastrophic events such as a large earthquake has long been recognized by emergency planners, financial organizations and the insurance industry. Using the AIR-Worldwide's earthquake model for Canada this paper presents a comprehensive study of the impact of a magnitude 9.0 Cascadia subduction zone earthquake (a 500 year return period event) on the Lower Mainland of British Columbia which is characterized by large accumulations of property and infrastructure exposed to high seismic hazard. The event also generates a relatively large tsunami affecting Vancouver Island and some regions in the greater Vancouver area. This paper provides an estimate of possible direct losses due to shaking, tsunami, liquefaction and landslide for buildings and infrastructures using high resolution (1km by 1km grid) inventory data. It is shown that the total direct losses not including business interruption and fire following can be as high as CAD 52 billion.

[1]Senior Engineer, Research and Modeling, AIR-Worldwide Corp., Boston MA, 02116
[2]Engineer, Research and Modeling, AIR-Worldwide Corp., Boston MA, 02116
[3]Senior Principle Engineer, Research and Modeling, AIR-Worldwide Corp., Boston MA, 02116

Nasseri A, Turel M, Yin Y and Lai T. Study of the impact of a magnitude 9 Cascadia subduction zone earthquake on British Columbia, Canada. *Proceedings of the 10th National Conference in Earthquake Engineering*, Earthquake Engineering Research Institute, Anchorage, AK, 2014

Tenth U.S. National Conference on Earthquake Engineering
Frontiers of Earthquake Engineering
July 21-25, 2014
Anchorage, Alaska

Study of the Impact of a Magnitude 9.0 Cascadia Subduction Zone Earthquake on British Columbia, Canada

A.Nasseri[1], M. Turel[2] , Y. Yin[2] and T. Lai[3]

ABSTRACT

The need for assessing potential impact of catastrophic events such as a large earthquake has long been recognized by emergency planners, financial organizations and the insurance industry. Using the AIR-Worldwide's earthquake model for Canada this paper presents a comprehensive study of the impact of a magnitude 9.0 Cascadia subduction zone earthquake (a 500 year return period event) on the Lower Mainland of British Columbia which is characterized by large accumulations of property and infrastructure exposed to high seismic hazard. The event also generates a relatively large tsunami affecting Vancouver Island and some regions in the greater Vancouver area. This paper provides an estimate of possible direct losses due to shaking, tsunami, liquefaction and landslide for buildings and infrastructures using high resolution (1km by 1km grid) inventory data. It is shown that the total direct losses not including business interruption and fire following can be as high as CAD 52 billion.

Introduction

A catastrophic event, such as an earthquake or a hurricane, can disrupt a nation's economic and social integrity. While natural disasters cannot be avoided, their impact can be assessed and mitigated. The primary step in evaluating the capacity of an urban society to manage disasters and to carry out an efficient recovery is to understand the risk and vulnerability of the system to catastrophes. In seismic prone regions such as Japan and the USA, the need for estimating possible losses due to future earthquakes has long been recognized by emergency planners, financial organizations and (re)insurance companies. AIR-Worldwide has developed earthquake loss estimation models for a number of counties around the globe that assimilate building inventory databases with hazard and vulnerability modules. Through probabilistic seismic analysis these model provide a basis for the aforementioned organization to make informed decisions in managing their risk.

The Lower Mainland of British Columbia is located in a region affected by complex tectonic plate boundaries. Despite the lack of significant damaging earthquakes in the past few

[1] Senior Engineer, Research and Modeling, AIR-Worldwide Corp., Boston MA, 02116
[2] Engineer, Research and Modeling, AIR-Worldwide Corp., Boston MA, 02116
[3] Senior Principle Engineer, Research and Modeling, AIR-Worldwide Corp., Boston MA, 02116

Nasseri A, Turel M, Yin Y and Lai T. Study of the impact of a magnitude 9 Cascadia subduction zone earthquake on British Columbia, Canada. *Proceedings of the 10th National Conference in Earthquake Engineering*, Earthquake Engineering Research Institute, Anchorage, AK, 2014

decades in this region, large magnitude earthquakes from the Cascadia subduction zone have occurred in history and are believed to be an inevitable threat in the future [1]. Furthermore, the region is characterized by the largest concentration of property values in Canada. The combination of seismic hazard and exposure concentration has rendered this area a high-risk region for financial organizations and the government. This paper presents an application of the AIR earthquake model for a scenario analysis in British Columbia and is part of a comprehensive study of economic and insurance impact of major earthquakes in Canada carried out for the Insurance Bureau of Canada (IBC) [2].

The scenario, a 1 in 500 year event, is a magnitude 9.0 earthquake caused by the Cascadia subduction zone which triggers a relatively large tsunami affecting Vancouver Island and the greater Vancouver area, parts of which are prone to liquefaction and landslide. The comprehensive study presented in the IBC report [2] provides estimates of potential direct and indirect economic (and insured) losses caused by shaking, tsunami, liquefaction, landslide and fire following using a high resolution property and infrastructure inventory database at a 1km by 1km grid. This paper presents the direct losses from all perils excluding fire following and business interruption. Maps showing the distribution and size of losses illustrate the impact of the event in the region. The next sections provide a brief description of seismic hazard in British Columbia, the selected scenario, the components of the model and the results of the study.

Seismic Hazard in British Columbia

The west coast of Canada is located in a region where interaction of several tectonic plates has created a unique seismic setting. This region is a part of the seismic belt in the Pacific Ocean, known as "the Ring of Fire". Off the west coast of Vancouver Island, the Juan de Fuca plate and the Pacific plate are spreading apart along the Juan de Fuca ridge. Further east, the Juan de Fuca plate is subducting beneath the North American plate to form the Cascadia subduction zone. Immediately north of this area is the Queen Charlotte fault, an active transform fault in which the plates are moving sideways in relation to one other.

An examination of the full history of earthquakes in the area clearly shows that the region is in fact seismically active. Figure 1 shows the tectonic setting and historical events in this region. According to Geological Survey of Canada the largest recorded onshore earthquake in Canada is the 1946 M7.3 earthquake on Vancouver Island which caused considerable damage. The event also triggered several landslides and many instances of liquefaction [3]. In 2001 a M6.8 earthquake in Nisqually, WA caused significant damage in the USA and was also greatly felt in Canada. This region has experienced some larger events with epicenters farther from the urban areas. One of those events is the 1949 M8.1 earthquake in Queen Charlotte Island. Another extremely large earthquake occurred in 1964 when an M9.2 tremor stuck Alaska and caused a devastating tsunami. The earthquake—the second largest earthquake in history—was felt in British Columbia, but no damage was caused by the shaking mainly due to the distance of the source. However, the tsunami caused notable damage in Port Alberni [4].

The most significant megathrust earthquake that has ever occurred at a relatively close distance to the British Columbia area is the M9.0 earthquake that hit the region in 1700. The event ruptured approximately 1000km of the fault in the Cascadia subduction zone from northern

Vancouver Island to northern California and spawned a large tsunami that travelled across the Pacific Ocean. According to the Natural Resources Canada (NRCan) the earthquake also triggered several landslides in Vancouver Island. The tsunami caused destruction in the Pacific coast of Japan and some villages in the Vancouver Island.

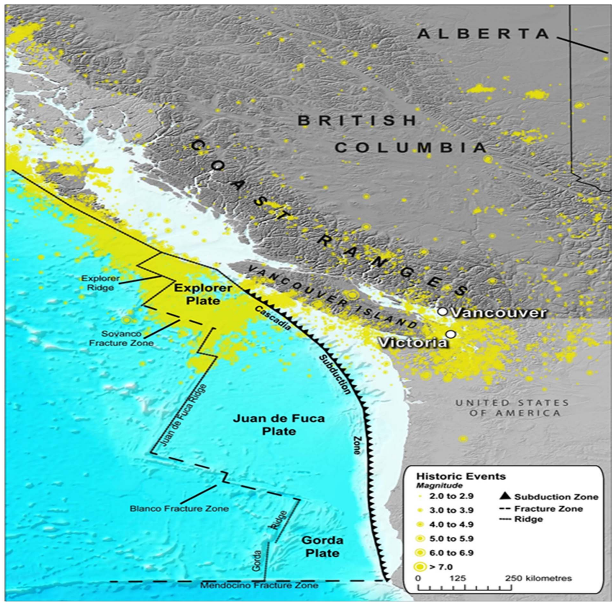

Figure 1. Historical earthquakes in British Columbia.

The Earthquake Scenario

Large subduction zone earthquakes of magnitude 8-9 have occurred at intervals of between 200 and 1000 years with an average return period of 500 years [1, 5]. The last occurred more than 300 years ago. In this study a similar earthquake is simulated and its consequences are investigated. The scenario is an M9.0 event occurring in the Cascadia subduction zone with an epicenter at a depth of 11km and approximately 75km off the west coast of Vancouver Island. The entire rupture extends from west offshore of central Vancouver island to offshore of central Oregon for about 840km (Figure 2a). The rupture consists of 14 fault segments with varying strikes and widths to fit the Cascadia subduction zone fault geometry. The width of the fault ranges from 86 km to 160 km. The average dip angle of the fault is 8 degrees and the coseismic slip on the rupture segments varies from 15 km to 40 km with a median slip of 20 km.

Ground Motion and Local Intensities

The first step in estimating damage and losses inflicted by the scenario is to determine ground motion intensity parameters such as peak ground acceleration (PGA) and spectral acceleration (at various periods) at all locations where there is a property at risk. Calculation of local intensity is done by applying ground motion prediction equations (GMPE) or attenuation relationships. The GMPEs provide ground motion intensity as a function of the magnitude, distance, and rupture mechanism of the earthquake. The intensity that a structure experiences at any given location is significantly affected by local site conditions which are often addressed through site amplification factors.

Researchers have studied and proposed various GMPEs for different types of seismic sources. For subduction zone events in the Cascadia subduction zone, the AIR model uses a weighted average of the GMPEs recommended by Atkinson and Goda [6]. These GMPEs include Atkinson and Boore, 2003 [7], Youngs et al., 1997 [8], Zhao et al., 2006 [9], Gregor et al., 2002 [10] and Atkinson and Macias, 2009 [11]. The weights used for combing these GMPEs are respectively, 0.2, 0.2, 0.4, 0.1 and 0.1. Figure 2a shows the ground motion intensity caused by the scenario earthquake, in terms of PGA.

(a) (b)

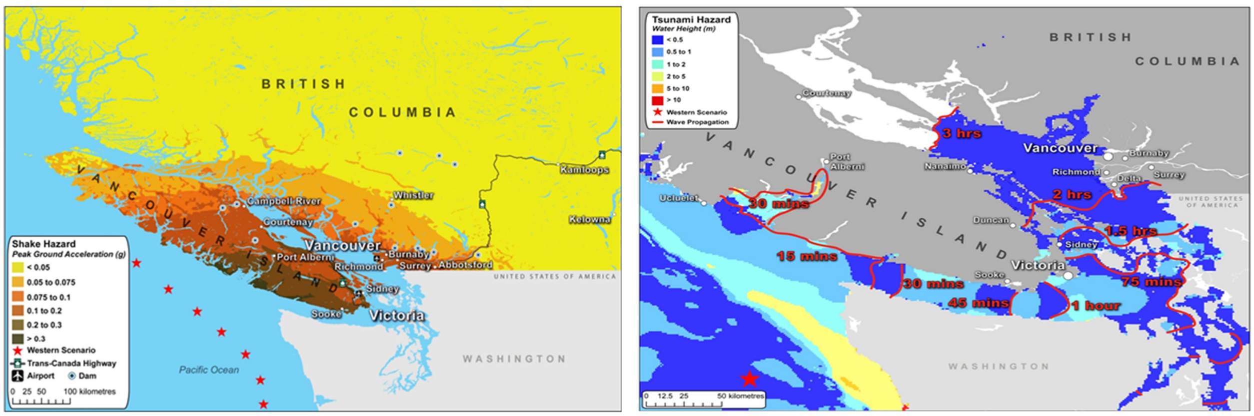

Figure 2. a: Peak ground acceleration. b: Tsunami height and timeline (red stars represents the centre of a fault patch ruptured in the earthquake)

Tsunami Simulation

As in the 1700 Cascadia earthquake, the scenario under study is capable of generating a relatively large tsunami. The AIR Earthquake Model for Canada employs a modified version of TUNAMI (Tōhoku University's Numerical Analysis Model for Investigation of Near-field tsunamis) [12] to perform tsunami simulations for events affecting Canada. It is a 2-D shallow water numerical grid-point model capable of simulating the propagation of a tsunami and modeling the inland extent of water. Taking into account the fault parameters, it generates an initial displacement of water surface and uses the method of deformation of an elastic half-sphere [13] and solves the mass and momentum equations of motion at specified time steps on an array of grid points (up to 125m resolution) using a finite difference strategy. Close to the shore, the effects of friction via a Manning coefficient are used to limit inundation.

Modification to the original TUNAMI model enables it to account for levees and their probabilistic failure and also the influence of spatially varying astronomical tides. The model provides solutions of water height and velocity at user-specified time intervals, along with maximum inundation height and current velocity which are used to estimate damage to buildings and infrastructures. Figure 2b shows the height and timeline of the tsunami waves. About 120 minutes after the rupture the tsunami wraps around Victoria with water heights about 1 to 2.5m in the western sections. After 150 minutes the tsunami wave has reached northern Vancouver with heights generally 1.0m or less. To the south of Vancouver, in an area extending from Bellingham to White Rock water levels above the background tide of 1.0 – 2.5 m are found over a widespread area.

Property and Infrastructure Exposure at Risk of Earthquake Damage

An essential part of AIR los s estimation models is a database containing the inventory of the properties at risk, including regular buildings and infrastructure, and an estimate of their replacement value. To compile the building inventory, detailed data (building counts, structural type, height classifications, and floor area) is gathered from a host of sources including government and private vendors. The primary sources of information used to derive the building counts are high resolution census data and business registries including ProCan B2B which are obtained through a private vendor (GEOGRAFX© Digital Mapping Service). Counts of businesses are obtained from the business registries along with the corresponding North American Industry Classification System (NAICS) codes that provide information about the type of business activity at each location. The CanVec dataset, produced by NRCan and distributed by GeoGratis, is the primary source of information for infrastructure. Additional regional datasets, such the Canadian Airport Charts diagrams from NAV CANADA and the Technical and Administrative Frequency Lists (TAFL) from Industry Canada, are also used.

Building replacement values are calculated using information about construction costs per square meter which vary by occupancy, construction type, height and location. Construction cost information is obtained from the Xactware® 360Value product, which provides component-based replacement cost estimates for rebuilding a particular structure and from construction cost guides and reports (e.g. published by Atlus Group and BTY Group). Valuations of infrastructure are based on data obtained from published reports and provincial data. They are benchmarked against the national economic accounts, which provided capital stock by province and by asset type (for more details and summary see [2]).

It is important to note that in the context of regional loss estimations it is not practical to analyze every individual building or infrastructure element. To keep the size and resolution of the problem on a manageable scale it is necessary to group the exposures in some reasonable geographical units. In this study buildings are classified based on their construction material, structural system, and building height. Exposure is presented at a 1km by 1km grid containing buildings of different construction type and occupancy classes (residential, commercial, industrial, etc.). Infrastructures are also considered at the same grid resolution with their values per unit length (in case of linear elements such as roads, pipelines, bridges etc.).

Seismic Vulnerability Module

Vulnerability functions correlate hazard intensity with expected damage as defined by the ratio of repair cost to replacement value. To provide a comprehensive damage estimation, the AIR model accounts for damage due to shaking and accompanying perils tsunami, liquefaction, landslide, and fire following earthquakes. Damage functions are commonly developed based on expert opinion, observational data, analytical studies, or a combination of these [14]. Observational method, which relies on the statistical analysis of data from post-earthquake damage surveys, and sometimes insurance claim data, is realistic but limited by the availability of data. The analytical approach synthesizes data for statistical analysis through structural analysis and overcomes the limitations of the observational method with regards to data availability and reliability. However, its effectiveness is curbed by modeling capabilities and computational costs. Damage functions in this study are developed with a hybrid approach, using both analytical and observational data.

Shaking Damage

Vulnerability functions for estimating damage due to ground shaking correlate mean damage ratios to some parameters representing the hazard intensity. In the past few decades researchers have used Modified Mercali Intensity [15, 16, 17] and PGA [18] as the hazard intensity measure. Knowing that damage is best correlated with building response, some studies presented damage function in terms of engineering demand parameters such as spectral acceleration(Sa) or spectral displacement(Sd) [19, 20].

Damage functions used in this study are presented in terms of spectral acceleration at different natural periods (Sa0.3 second for low-rise, Sa1.0 second for mid-rise and Sa3.0 second for high-rise buildings). Nonlinear dynamic analysis (NDA) of the mathematical models representing different building types subjected to a large ensemble of ground motion is extensively used for two purposes. It is used to establish relationships between maximum interstory drifts and ground motion parameters and to develop vulnerability functions in terms of engineering demand parameters which are then converted spectral acceleration using the already established relationships. Observational data from Northridge 1994, Loma Prieta 1989, and L'Aquila 1999 earthquake are used in generating and validating the damage functions for wood and masonry structures. In addition, studies of the seismic vulnerability of buildings in Canada [17, 21] are used to validate the damage functions.

Similar to the approach used in HAZUS, the vulnerability of buildings of the same type and height is further classified in to five levels based on their expected seismic resistance. These vulnerability classes are defined in terms of seismic code levels which reflect the degree of scrutiny used in design and construction of these buildings. Accordingly, damage functions are presented for the five vulnerability classes of "pre code" (e.g. building with no seismic design), "low code" (e.g. buildings designed to early version of seismic codes), "moderate code", "high code" and "special code"(e.g. buildings designed to the most recent codes in seismic regions) in the descending order of vulnerability. For more information about the uniform vulnerability assessment framework used in this study refer to [22]. Figure 3a shows an example of damage functions for low-rise reinforced concrete (RC) frame structures.

Tsunami Damage

Tsunami damage is caused by a combination of hydrostatic forces (related to water depth), hydrodynamic forces (related to flow velocity), and debris collision and buoyancy forces that wash the buildings away and turn them into new debris. In a broader aspect, tsunami damage can also include soaking, scouring by sand or other sediments against surfaces, sedimentation, and chemical contamination.

Tsunami damage functions in the AIR Earthquake model are developed empirically using a large set of observational data from the 2010 Tōhoku earthquake and the 2004 Indonesia earthquake. In addition, studies from Japan's Ministry of Land, Infrastructure, Transport and Tourism (MLIT) [23] and [24] were used in developing relationships between the tsunami inundation and flow velocity in generating the damage functions. Taking into account the inundation depth and flow velocity, the vulnerability functions explicitly account for the hydrostatic, hydrodynamic and buoyancy forces. Other factors such as soaking, scouring, contamination, and sedimentation are implicitly accounted for in the damage estimates as the data used to develop the damage functions include the impact of these sources. Moreover, the effect of debris on building damage is accounted for through empirically developed debris functions for buildings of different construction type and height. At very shallow depths (<0.5 m), usually there is no or little impact from the debris. Increased inundation height intensifies the buoyancy forces causing an increase in the size and amount of debris. The debris effect increases with inundation only up to a point; it falls off at higher inundation levels where the building is already damaged and the debris does not cause further damage. Figure 3b shows an example of tsunami damage functions for low rise RC buildings

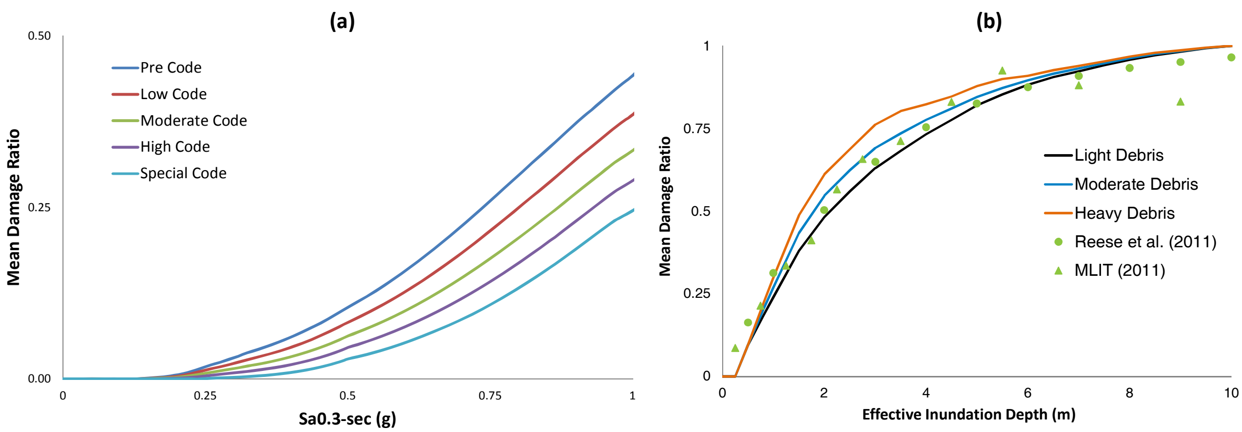

Figure 3. a: Damage functions for low rise RC buildings of different seismic code design b: Tsunami damage functions for low rise RC buildings

Liquefaction and Landslide Damage

As highlighted by recent earthquakes in New Zealand (2010 and 2011) and in Japan (2011), ground failure can make a significant contribution to overall losses in an earthquake event. In a comprehensive loss estimation study it is imperative to include the losses from these perils. Unlike shake damage, which often occurs in a vast area, ground failure is localized to areas that are prone to the hazard. Estimating losses from ground failure in a regional model requires detailed information about the physical properties of the affected area.

Liquefaction occurs when pore water pressure increases due to ground shaking and causes the soil to lose stiffness and accumulate permanent ground displacement. Development of a regional liquefaction module relies on the strong correlation that exists between liquefaction susceptibility and surficial geology. In this study published surficial geology and liquefaction hazard maps and water well data are compiled from NRCan and provincial sources. The liquefaction estimation method used in the model, which compares liquefaction resistance to liquefaction demand, follows collective research summarized in [25]. Liquefaction resistance is defined by soil strength characterized with shear-wave velocity, soil type, and groundwater depth, while liquefaction demand is a function of ground motion intensity. Representative soil profiles are assigned to each region following an examination of all available shear-wave velocity profile data from different sources [26]. Building damage resulting from liquefaction is modeled as a function of permanent ground displacement (PGD) due to post-liquefaction reconsolidation settlement. PGD is determined using the relationship between factor of safety and volumetric strain proposed by [27]. Liquefaction vulnerability functions are developed by leveraging damage functions in HAZUS in light of liquefaction damage data from the recent Japan and New Zealand earthquakes.

Earthquake-triggered landslides can also cause significant damage to buildings and infrastructure. The susceptibility of an area to landslides can be assessed based on potential ground motion, and geological and topographical conditions. A regional landslide module (GIS based) requires input from Digital Elevation Model (DEM) data, surficial and bedrock geological maps, and seasonal precipitation data. DEM information (obtained from Canadian Digital Elevation Data, CDED) is used to create slope maps, while surficial and bedrock geological maps are used to classify geological units based on their material strength. Precipitation data is used to estimate seasonal fluctuations in water saturation of soils which affects the stability of slopes. A simplified process-based module that relies on the infinite slope stability method coupled with Newmark's displacement method was used [28]. Strength parameters are assigned to each map unit following an examination of the bedrock and surficial geological maps. From the ground motion parameters of the scenario earthquake the permanent ground displacement is determined for each grid cell. Utilizing the vulnerability function from HAZUS, damage to buildings and infrastructure is estimated using the calculated PGD. Figure 4 shows the landslide and liquefaction hazard maps for the scenario earthquake.

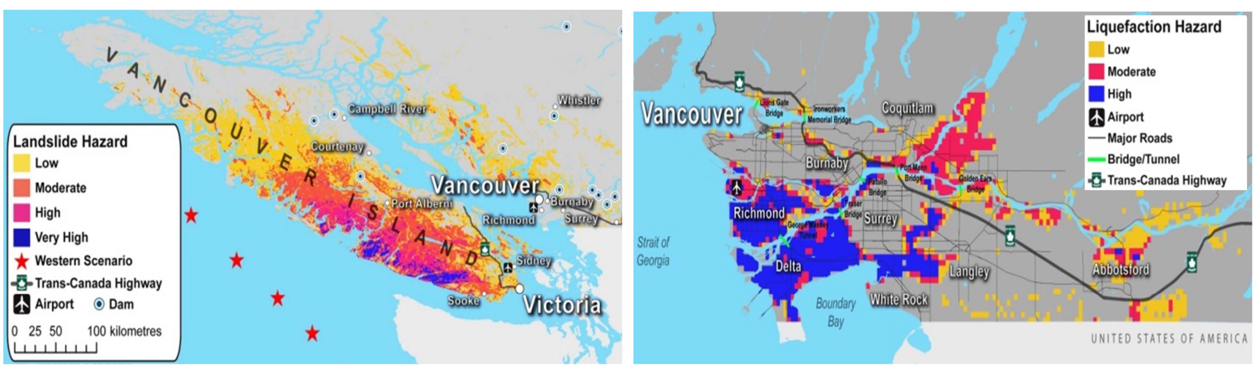

Figure 4. Liquefaction and landslide hazard maps for the scenario earthquake

Results

Results of the simulation are presented in terms of damage ratio footprints and the expected losses for buildings and infrastructure. Damage ratio footprints conveniently demonstrate the extent and severity of the damage in the affected regions and show where certain perils may have greater impact. Information presented in these footprints can be used by public safety and emergency planners to identify regions that need attention and to make strategic decisions about dispatching emergency or safety investigation units and ultimately for repair and reconstruction. The total amount of losses in the affected area is presented for regular properties and infrastructure with a break down of different types in each category.

It must be noted that damage ratios shown here reflect the combined damage caused by all perils. Since damage for each peril is calculated independent of other perils, it is important to consider the probability of overlapping when calculating the total damage. The merging scheme adopted here is one that considers the probability of the overlapping based on the severity of the damage from each peril. The probability is defined empirically presuming no overlap when the sum of damage ratios is smaller than 10% sigmoid increase to 1.0 when the sum exceeds 60%. Once the overlapping is determined, the final damage ratio is calculated as the sum minus the overlap defined in Eq.1. In this equation DR_o is the overlap, DR_i is damage ratio of peril i and p is the probability of overlapping.

$$\mathrm{DR_O} = \mathrm{p}(\mathrm{O_{max}} + \mathrm{O_{min}})/2 \tag{1}$$

$$\mathrm{O_{max}} = \sum_{i=1}^{n} \mathrm{DR_i} - \max(\mathrm{DR_i}) \quad ; \quad \mathrm{O_{min}} = \max(0, \sum_{i=1}^{n} \mathrm{DR_i} - 1) \tag{2a,b}$$

Figure 5 shows the damage ratio for buildings and infrastructure. Each pixel represents an average damage at a 1km grid. As can be seen in Figure 5a, damage extends from east of Abbotsford to north of Vancouver Island. Not surprisingly, larger damage is concentrated in areas closer to the rupture such as the south west of greater Vancouver and around Victoria. Figure 5b demonstrates that infrastructure damage is large and widespread around Victoria and in Richmond and Delta. Transportation system (highways, bridges and tunnels) suffer the largest damage followed by airports and the electrical transmission system.

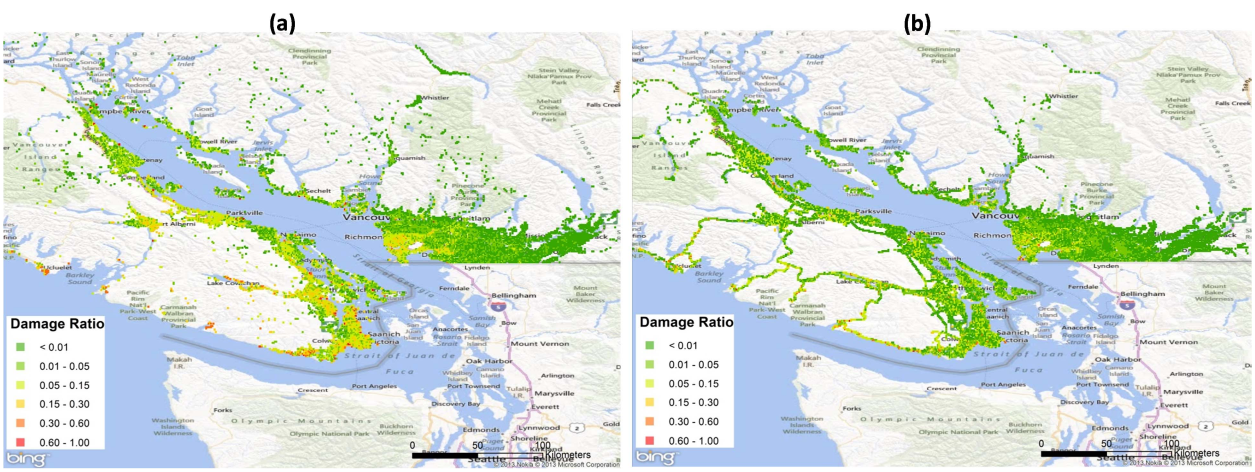

Figure 5. Damage footprints. a: Regular properties. b: Infrastructures

Damage caused by liquefaction and tsunami is shown in Figure 6. Areas on the Fraser River delta such as the cities of Richmond, Delta and Surrey are located on Holocene sediments and are at a particular risk of liquefaction. As illustrated in Figure 6a, significant liquefaction damage is expected in these regions. Notable landslide damage is anticipated for property and infrastructure in the elevated parts of Vancouver Island. Liquefaction and landslide collectively contribute 9% and 40% of total losses respectively for property and infrastructure.

Figure 6b shows damage caused by tsunami waves. Some moderate to large damage is anticipated along the eastern coast of Vancouver Island. The red spots show the regions where tsunami is likely to cause extensive damage. Overall, tsunami contributes 7.1% and 4.8% of the total losses for property and infrastructure respectively. Table 1 and 2 summarize the losses by peril and by type for property and infrastructure respectively. The total direct loss from this scenario is 53.65 billion CAD. It is necessary to note that for the sake of brevity fire following earthquake and business interruption are not addressed here. When these losses are added, the total direct loss reaches 62 billion CAD [2].

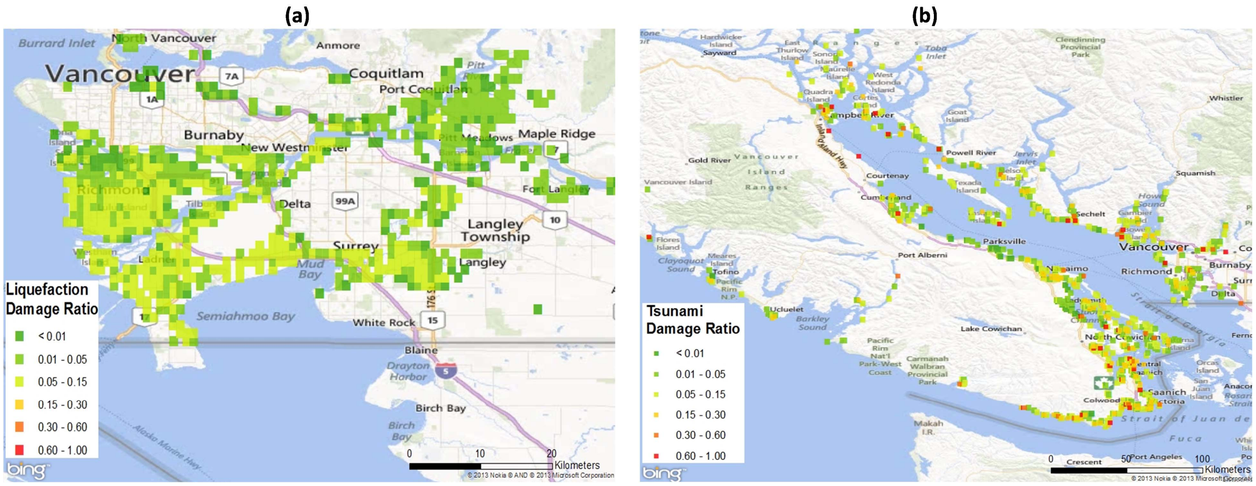

Figure 6. a: Liquefaction damage in the greater Vancouver area. b: Tsunami damage

Table 1. Summary and break down of losses in building properties

Type of property	Loss (in million CAD)		
	Shake	Tsunami	Liquefaction / Landslide
Residential	18,838	2,270	2,277
Commercial/Industrial	24,479	1,280	1,973
Agricultural	93	5	32
Automobiles	199	238	79
Total	43,609	3,792	4,361
	Total direct loss *		51,763

* Does not include losses due to fire following earthquake and losses due to business interruption

Conclusions

The study reported here contemplates a major plausible earthquake from the Cascadia subduction zone. The magnitude 9.0 event, which represents a 500 year return period event, triggers a relatively large tsunami and causes liquefaction and landslide damage. Although not a prediction of any future event, the results shown in this study provide a picture of the possible impact that such an event can have in the Lower Mainland of British Columbia. The widespread damage to property and infrastructure extends from east of Abbotsford to the north west of Vancouver Island. Potential liquefaction damage, particularly to infrastructure, is highlighted in liquefaction prone areas of the Fraser River delta. The tsunami is shown to have a noticeable contribution to the total damage and losses, particularly in the coastal areas of Vancouver Island and south of greater Vancouver. The estimated direct losses of 52 billion CAD for property and 1.89 billion CAD for infrastructure (excluding fire following and business interruption) are alarming costs that underscore the need for proper planning for mitigation and financial recovery.

Table 2. Summary and break down of losses in infrastructure

Type of infrastructures	Loss (in million CAD)		
	Shake	Tsunami	Liquefaction / Landslide
Transportation-Roads	260.7	61.6	255.9
Transportation-Railways	63.5	2.3	26.6
Airport	239.5	-	77.8
Port	173.3	17.0	70.7
Pipeline-oil	39.6	0.1	186.3
Pipeline-water	0.0	-	1.2
Pipeline-Gas	21.9	0.1	90.2
Electrical transmission/Telecom	245.4	9.7	44.4
Total	1,043.9	90.8	753.1
	Total direct loss *		1,887.8

* Does not include losses due to fire following earthquake and losses due to business interruption

Acknowledgments

The authors would like to thank the support from the Insurance Bureau of Canada and collaboration of the Exposure, Seismic Hazard and Tsunami Hazard teams at AIR-Worldwide.

References

1. CREW, 2013. "Cascadia subduction zone earthquakes: a magnitude 9 earthquake scenario" Cascadia Region Earthquake Workgroup. http://crew.org/sites/default/files/cascadia_subduction_scenario_2013.pdf
2. AIR-Worldwide, 2013. "Study of the impact and the insurance and economic cost of a major earthquake in British Columbia and Ontario/Quebec", *report for the Insurance Bureau of Canada*. http://www.ibc.ca/en/Natural_Disasters/documents/IBC_EQ_Study_Full.pdf
3. Cassidy, J.F., Rogers, G.C., Lamontagne, M., Halchuk, S., Adams, J., 2010. "Canada's earthquakes: the good the bad and the ugly", *Geosceience Canada* **37** (1): 1-16.
4. Lamontagne, M., Halchuk, S., Cassidy, J.F., Rogers, G.C. 2008. "Significant Canadian Earthquakes of the period 1600-2006", *Seismological Research Letters*, **79**: 211-223.
5. Mazzotti, S., and Adams, J., 2004. "Variability of near-term probability for the next great earthquake on the Cascadia subduction zone", *Bulletin of the Seismological Society of America*, **94** (5): 1954-1959.
6. Atkinson, G. M., and Goda, K., 2011. "Effect of Seismicity Models and New Ground-Motion Prediction Equations on Seismic Hazard Assessment for Four Canadian Cities," *Bulletin of Seismological Society of America*, **101**: 176–189.
7. Atkinson, G. M., and Boore, D.M., 2003. "Empirical ground motion relations for subduction zone eartqhaukes and their application to Cascadia and other regions", *Bulletin of Seismological Society of America*, **93** (4): 1703-1729.
8. Youngs, R. R. , Chiou,S.J., Silva, W. J., Humphrey, J. R., 1997. "Strong ground motion attenuation relationships for subduction zone earthquakes". *Seismological Research Letters*, **68**(1):58–73.
9. Zhao J. X., Zhang, J., Asano, A., Ohno, Y., Oouchi, T., Takahashi, T., Ogawa, H., Irikura, K., Thio, H., Somerville, P., Fukushima, Y., 2006. "Attenuation Relations of Strong Ground Motion in Japan Using Site Classification Based on Predominant Period," *Bulletin of the Seismological Society of America*, **96**: 898–913.

10. Gregor, N. J., Silva, W. J., Wong, I. G., Youngs, R.R., 2002. "Ground motion attenuation relationships for Cascadia subduction zone megathrust earthquakes based on a stochastic finite-fault model", *Bull. Seismol. Soc. Am.* **92**: 1923–1932.
11. Atkinson, G. M., Macias, M., 2009. "Predicted Ground Motions for Great Interface Earthquakes in the Cascadia Subduction Zone," *Bulletin of Seismological Society of America*, **99**: 1552–1578.
12. Imamura, F., and others, 2011. "The Tōhoku region Pacific earthquake and tsunami simulation model", Tōhoku University. Available from: http://www.tsunami.civil.Tōhoku.ac.jp/hokusai3/J/events/Tōhoku_2011/model/dcrc_ver1.1_111107.pdf
13. Okada, Y., 1985. "Surface deformation due to shear and tensile faults in a half-space", *B. Seismol. Soc. Am.*, **75**: 1135–1154.
14. Rossetto, T. and Elnashai, A., 2003, "Derivation of Vulnerability Functions for European-type RC Structures Based on Observational Data," *Engineering Structures*, **25**: 1241-1263.
15. Applied Technology Council 1985, "Earthquake Damage Evaluation Data for California," *ATC-13*, funded by Federal Emergency Management Agency.
16. Grünthal, G., Musson, R. M. W., Schwarz, J., Stucchi, M., 1998. "European Macroseismic Scale 1998 (EMS-98)" *report of the European Seismological Commission*, Subcomission on Engineering Seismology, Working Group Macroseismic Scales.
17. Ventura, C.E., Finn, W.D.L., Onur, T., Blanquera, A., and Rezai, M. 2005. "Regional seismic risk in British Columbia — classification of buildings and development of damage probability functions", *Canadian Journal of Civil Engineering*, **32**: 372–387.
18. Rota M., Penna, A., and Strobbia, C.L., 2008, "Processing Italian Damage Data to Derive Typological Fragility Curves," *Journal of Soil Dynamics and Earthquake Engineering*, **28**: 933-947.
19. DHS-FEMA, 2003. "Multi-hazard loss estimation methodology: HAZUS MR4 technical manual". National Institute of Building Sciences, Washington DC.
20. RISK-UE 2001, "An Advanced Approach to Earthquake Risk Scenarios with Applications to Different European Towns - WP1 Report European Distinctive Features, Inventory Database and Typology," *report by the European Commission*, 2001.
21. Onur, T., Ventura, C.E., Finn, W.D.L., 2005. "Regional seismic risk in British Columbia- damage and loss distribution in Victoria and Vancouver", *Canadian Journal of Civil Engineering*, **32**: 361–371
22. Lai, T., Nasseri, A., Katiyar, V., Tang, Y, Guin, J., Towashiraporn, P., 2012. "A uniform framework of seismic vulnerability assessment and its application in seismic risk analysis of European countries", *proceedings of the 15the WCEE*, Lisbon, Portugal 2012.
23. Ministry of Land, Infrastructure, Transport, and Tourism (MLIT), 2011, "Status survey results affected by the earthquake east, in Japanese". http://www.mlit.go.jp/report/press/toshi07_hh_000056.html.
24. Reese, S., Bradley, B.A., Bind, J., Smart, G., Power, W., Sturman, J., 2011, Empirical building fragilities from observed damage in the 2009 South Pacific tsunami, *Earth-Science Reviews*, **107**:156-173.
25. Idriss, I. M. and Boulanger, R.W., 2008. "Soil liquefaction during earthquakes," *Monograph MNO-12*, Earthquake Engineering Research Institute, Oakland, California.
26. Hunter, J. A., Burns, R.A., Good, R.L., Pelletier, C.F., 1998."A compilation shear wave velocities and borehole geophysical logs in unconsolidated sediments of the Fraser River delta", *Open File 3622, Geological Survey of Canada*, Ottawa, Canada.
27. Ishihara, K. and Yoshimine, M., 1992, "Evaluation of settlements in sand deposits following liquefaction during earthquakes," *Soils and Foundations*, **32**: 173–188.
28. Wilson, R.C., and Keefer D.K., 1985, "Predicting Areal Limits of Earthquake Induced Landsliding, Evaluating Earthquake Hazards in the Los Angeles Region", *U.S. Geological Survey Professional Paper*, 317-493.